Molecular Cancer Therapeutics

An Antibody Targeted to VEGFR-2 Ig Domains 4-7 Inhibits VEGFR-2 Activation and VEGFR-2–Dependent Angiogenesis without Affecting Ligand Binding

Jane Kendrew[1], Cath Eberlein[1], Brad Hedberg[2], Karen McDaid[1], Neil R. Smith[1], Hazel M. Weir[1], Stephen R. Wedge[1], David C. Blakey[1], Ian Foltz[2], Joe Zhou[2], Jaspal S. Kang[2], and Simon T. Barry[1]

Abstract

Inhibition of VEGFR-2 signaling reduces angiogenesis and retards tumor growth. Current biotherapeutics that inhibit VEGFR-2 signaling by either sequestering VEGF ligand or inhibiting VEGF binding to VEGFR-2 may be compromised by high VEGF concentrations. Here we describe a biotherapeutic that targets VEGFR-2 signaling by binding to Ig domains 4-7 of VEGFR-2 and therefore has the potential to work independently of ligand concentration. 33C3, a fully human VEGFR-2 antibody, was generated using XenoMouse technology. To elucidate the mechanism of action of 33C3, we have used a number of competition and binding assays. We show that 33C3 binds VEGFR-2 Ig domains 4-7, has no impact on VEGF-A binding to VEGFR-2, and does not compete with an antibody that interacts at the ligand binding site. 33C3 has a high affinity for VEGFR-2 (K_D < 1 nmol/L) and inhibits VEGF-A induced phosphorylation of VEGFR-2 with an IC_{50} of 99 ± 3 ng/mL. *In vitro*, in a 2D angiogenesis assay, 33C3 potently inhibits both tube length and number of branch points, and endothelial tubule formation in a 3D assay. *In vivo*, 33C3 is a very effective inhibitor of angiogenesis in both a human endothelial angiogenesis assay and in a human skin chimera model. These data show targeting VEGFR-2 outside of the ligand binding domain results in potent inhibition of VEGFR-2 signaling and inhibition of angiogenesis *in vitro* and *in vivo*. *Mol Cancer Ther; 10(5); 770–83. ©2011 AACR.*

Introduction

The VEGF-A plays a critical role in inducing vascular growth and remodeling during development, and in a number of pathological conditions including driving the angiogenic response required to support solid tumor growth. VEGF-A signaling is predominantly mediated through activation of VEGF receptor 2 (VEGFR-2; KDR/flk-1), which stimulates endothelial cell proliferation, migration, vascular permeability, and neovascular survival (1). Sequestering VEGF-A, or inhibiting VEGFR mediated signaling gives therapeutic benefit in a range of preclinical tumor models through targeting the tumor vasculature. Various agents that target VEGFR mediated signaling have been developed. These agents fall into 3 classes. Firstly, the VEGF-A ligand sequestering agents such as bevacizumab and aflibercept (2,3). Secondly, small molecular weight tyrosine kinase inhibitors (TKI) such as PTK787, Sutent, sorafinib, Zactima, and Recentin, (4–8). Lastly, antibody or antibody like molecules that block the interaction of VEGF-A with VEGFR-2 such as IMC1121b and CDP-791 (9,10).

VEGFR-2 is a member of a broader family of receptor tyrosine kinases consisting the VEGFR1, 2, and 3 also known as flt-1, KDR, and flt-4. This is a family of transmembrane tyrosine kinase receptors with 7 Ig domains. Ligands such as VEGF-A and placental growth factor bind the VEGFRs within immunoglobin-like domains 2 and 3, with domain 2 making the primary contact and domain 3 determining the specificity of binding (11,12). In contrast, Ig domains 4-6 are involved in dimerization of the receptor complexes, with dimerization and transphosphorylation required to generate downstream signaling, enabling sustained signaling to proceed. As receptor activation is a function of both binding and dimerization, in theory, receptor activation, and productive signaling can be inhibited by inhibiting ligand–receptor binding or by blocking dimerization. Inhibiting VEGFR-2 signaling through inhibition of dimerization provides a novel mechanism for inhibition of VEGFR-2 signaling similar to a small molecule TKI. However, small molecule TKIs are not selective for VEGFR-2, and often inhibit other kinases, which can lead to additional toxicities, especially when used in combination with other broad spectrum inhibitors. Neutralizing VEGF-A signaling by either ligand sequestration or ligand blockade can

Authors' Affiliations: [1]Cancer Bioscience, AstraZeneca Pharmaceuticals, Alderley Park, Macclesfield, Cheshire, United Kingdom; and [2]Amgen (formerly Abgenix), Burnaby, British Columbia, Canada

Corresponding Author: Simon T. Barry, Cancer and Infection Research, AstraZeneca, Mereside, Alderley Park, Macclesfield, Cheshire, SK10 4TG, United Kingdom. Phone: 44-1625-513350; Fax: 44-1625-513624. E-mail: Simon.T.Barry@astrazeneca.com

doi: 10.1158/1535-7163.MCT-10-0876

be impacted by the concentration of ligand, and in some cases may lead to lack of suppression of ligand on chronic administration.

We therefore hypothesized that a therapeutic antibody targeting the Ig 4-7 domains of VEGFR-2 would be able to deliver therapeutic benefit independent of ligand concentration and would represent a differentiated mode of action for targeting VEGFR-2 signaling. Here we describe the generation of a fully human therapeutic antibody, 33C3, targeting VEGFR-2 and its effects in model systems mimicking angiogenesis *in vitro* and *in vivo*.

Materials and Methods

Reagents

Recombinant VEGF-A, isotype controls, and Aprotonin were purchased from Sigma. VEGFR-2 extracellular domain (ECD)/Fc/His chimera, mouse anti-polyhistidine horseradish peroxidase (HRP), peroxide/tetramethyl benzidine (TMB) substrate and stop solution were purchased from R&D Systems. Cytodex 3 beads were purchased from GE Healthcare and rehydrated in PBS to give 60,000 beads per mL. Fibrinogen and bovine derived thrombin, were obtained from Calbiochem. CD31 (PECAM-1) Alexa Fluor 488 Anti Human Clone M89D3 Isotype Mouse IgG2a kappa was purchased from Becton Dickinson. For immunohistochemistry analysis a mouse monoclonal antibody specific to human CD31 (JC70A, Dako), rabbit polyclonal antibody detecting mouse and human CD31 (CHG-CD31-P1; generated in house at AstraZeneca) and rabbit monoclonal to human VEGFR-2 (55B11; CST) were used.

Cell culture

Porcine aortic endothelial (PAE) cells were obtained from the Ingrid Schiller Ludwig Institute for Cancer Research. No further authentication was done. A PAE line stably overexpressing human VEGFR-2 under the control of a SV40 promoter was subsequently generated (PAE-VEGFR-2). Cells were cultured in Hams F12 media supplemented with 10% serum and maintained in 5% CO_2 at 37°C. Primary human umbilical vein endothelial cells (HUVEC), primary normal human dermal fibroblasts and culture media were purchased from Promocell. Each vial of primary cells was used for no more than 6 passages. Cells were maintained in 5% CO_2 at 37°C. Angiogenesis kits and tubule staining kits were obtained from TCS CellWorks Ltd. and processed as described in the manufacturer's protocol with antibody titrations prepared in MCDB131 media (Invitrogen) supplemented with 2% serum and 11.6 mmol/L L-glutamine.

Immunization and antibody generation

Antibodies to VEGFR-2 were generated using XenoMouse as described in US patent application serial number 08/759,620 and International patent Applications WO98/24893 and WO00/76310. Animals were immunized with soluble VEGFR-2 ECD, domains 1-7 (Calbiochem). Ten milligram per mouse was used for the initial injection followed by boosts of 5 mg/mouse every week for 6 weeks. Titres of antibody against human VEGFR-2 were followed by fluorescence-activated cell sorting (FACS) using HUVECs and by ELISA to recombinant soluble human VEGFR-2 domains 1-7. Spleens were harvested from the mice showing the strongest titres and hybridomas generated by B cell fusion with myeloma P3 × 63Ag8.653 cells purchased from the American Type Culture Collection (catalogue no. CRL1580) as described (13).

Recombinant VEGFR-2 binding assays

To show that 33C3 binds to the dimerization region of VEGFR-2, full length, and a fragment corresponding to Ig domains 4-7 of the receptor were used in binding assays. His/FC tagged VEGFR-2 domains 4-7 were cloned and overexpressed in HEK 293T cells producing a VEGFR-2 Ig 4-7 ECD/Fc/polyhistidine chimera. The protein fragment was isolated by passing cell supernant over a nickel column. To assay binding of protein to immobilized antibodies dilutions of isotype control IgG, 33C3 or VEGF receptor–ligand binding (VRLB) antibody was prepared in PBS and incubated in replicate 96-well microtiter plates. The precoated plates were washed 2 times with PBS and blocked with PBS containing 3% bovine serum albumin (BSA) for 1 hour at room temperature. The plates were washed 3 times with PBS and incubated for 1 hour at room temperature on an orbital shaker with either c. 10 μg/mL VEGFR-2 (4–7) ECD/Fc or 10 μg/mL full length VEGFR-2 (1–7) ECD/Fc (R&D Systems) in PBS. The plates were washed 3 times with PBS and incubated with anti-polyhistidine-HRP for 1 hour at room temperature. The plates were washed again with PBS and the substrate for HRP was added and the reaction stopped after 15 minutes incubation at room temperature. The optical density (OD) 450 nm was read to quantify the plate bound VEGFR-2 protein fragments.

To assay binding of antibodies to immobilized VEGFR-2 Ig domains 4-7, His-tagged VEGFR-2 domains 4-7 (c. 10μg/mL PBS) was used to coat 96-well microtitre plates overnight at 4°C. The precoated plates were washed with PBS and blocked with PBS containing 3% BSA for 1 hour at room temperature. The plates were washed 3 times with PBS and incubated for 1 hour at room temperature on an orbital shaker with dilutions of isotype control IgG, 33C3, or VRLB prepared in PBS. Bound antibody was detected as described above.

Cross-competition assay to define 33C3 binding domain on recombinant VEGFR-2, murine VEGFR-2, and VEGFR-1

To assess competitive binding of 33C3, soluble biotinylated VEGFR-2 was captured on neutravidin coated plates and the competitor agents were used to prevent binding of 33C3. 96-well plates (Costar) were coated with neutravidin (Pierce) overnight in PBS (0.05% azide). The following morning plates were washed with PBS and blocked with PBS 1% milk for 1 hour at room temperature. Plates were then washed again and incubated with

1 μg/mL biotinylated recombinant VEGFR-2 (Calbiochem) for 1 hour at room temperature. To compete for 33C3 binding to the captured VEGFR-2, 33C3 (0.1 μg/mL) was preincubated for 1 hour at room temperature with VEGFR-1 (R&D Systems; 5 μg/mL), murine VEGFR-2 (5 μg/mL; R&D Systems), full length VEGFR-2 (5 μg/mL) and VEGFR-2 Ig domains 4-7 (25 μg/mL), before addition to the assay plate. All incubations with 33C3 were performed in PBS 1% milk. 33C3 (± competitors) was allowed to bind to immobilized VEGFR-2 for 1 hour at room temperature and then the plates were washed extensively. Binding of 33C3 was then detected using a goat anti-human IgG Fc HRP conjugate at 400 ng/mL, again incubated for 1 hour at room temperature. Following bond antibody was visualized using 1 step TMB (Neogen) and plates read OD at 450 nm.

Affinity measurement

A solution phase BIAcore procedure was used to determine the affinity of 33C3 for VEGFR-2. 33C3 was immobilized on a CM4 sensor chip within a BIAcore 2000 using standard amine coupling. VEGFR-2 was diluted to a starting concentration of 52 nmol/L and tested in a 3-fold dilution series in triplicate. The running buffer contained HBS-P (0.01 mol/L HEPES, 0.15 mol/L NaCl, 0.005% Tween-20, pH 7.4) with 0.1 mg/mL BSA and binding responses were collected at 23°C. Bound complexes were regenerated with a 12 second pulse of 1/100 dilution of phosphoric acid. The response data were globally fit with a simple 1:1 interaction model and a value for K_D was estimated.

Cell based VEGFR-2 FACS binding assay

Binding of 33C3 to cell expressed VEGFR-2 was determined by FACS. PAE-huVEGFR-2 cells grown to 90% confluency were trypsinized and washed in 50 mL of full media. The cells were then counted and pelleted at 1000 rpm for 5 minutes. The cells were washed in a further 50 mL of ice cold PBS/1% BSA repelleted at 1000 rpm for 5 minutes and resuspended in ice cold PBS/1% BSA at 2.5×10^6 cells per mL. For each assay point 200 μL of cell suspension was used, with 33C3 or control IgG antibodies added at different concentrations. The samples were incubated on ice for 1 hour, washed twice with 4 mL of ice cold PBS/1% BSA per sample. Between each wash the cells were pelleted at 1000 rpm for 5 minutes. Following the second wash the cells were resuspended in 200 μL of ice cold PBS, anti-human ALEXA 488 secondary added at a 1 in 200 dilution and incubated for 1 hour on ice. The samples were washed twice with 4 mL of ice-cold PBS/1% BSA as above. The final samples were resuspended in 500 μl of PBS and antibody binding analyzed using the FACS Caliber.

Cell based antibody cross-competition binding assay

Differential epitope binding of the VEGFR-2 antibodies was measured by competition binding. 96-well microtitre plates were coated with a fixed concentration of VEGFR-2 antibody, at 1 μg/mL PBS, overnight at 4°C. The plates were washed and blocked with PBS containing 3% BSA for 1 hour at room temperature. Titrations of each antibody were prepared in serum free Hams F12 media at 10× the final assay concentration. Meanwhile PAE-VEGFR-2 cells were trypsinized and washed in 50 mL of serum free Hams F12 media. The cells were counted and resuspended at 100,000 cells per 90 μL of serum free Hams F12 media. The coated plates were washed twice with PBS and 10 μL of antibody dilution added in triplicate wells. 100,000 PAE-VEGFR-2 cells were added per well and the plates incubated at 37°C, 5% CO_2 for 1 hour. Following incubation any nonadhered cells were flicked from the plates and each well washed carefully 3 times with PBS. The adhered cells were fixed with ethanol for 30 minutes at room temperature. The ethanol was tipped off the plates and the cells stained with 0.1% crystal violet solution in 1.5% methanol. After 15 minutes incubation the crystal violet was washed off and the stain solubilized with a solution of 0.1% Triton X-100 in double distilled water and incubation at room temperature for 2 hours on an orbital shaker. The OD 570 nm was read and the data plotted.

VEGF-A/VEGFR-2 blocking assay

The impact of VEGFR-2 antibodies on VEGF-A/VEGFR-2 binding was measured using a VEGF-A blocking assay. Various amounts of antibody were mixed with a fixed amount of VEGFR-2 ECD/Fc/polyhistidine chimera (500 ng/mL) and incubated at room temperature for 2 hours. Meanwhile 96-well microtiter plates precoated with VEGF-A (5 ng/well) were washed 2 times with PBS and blocked with PBS containing 3% BSA for 2 hours at room temperature. The plates were washed 3 times with PBS and the antibody mixtures then transferred to the plate and incubated overnight at 4°C on an orbital shaker. The plates were washed 3 times with PBS and incubated with anti-polyhistidine conjugated with HRP for 2 hours at room temperature. The plates were washed with PBS and the substrate for HRP was added and the reaction stopped after 15 minutes incubation at room temperature. The OD 450 nm was read to quantify the plate bound VEGFR-2 ECD and the IC_{50} values calculated.

Receptor phosphorylation assays

Potency of the VEGFR-2 blocking antibodies was determined using PAE-VEGFR2 cells or HUVECs. Cryopreserved PAE cells, stably transfected with a VEGFR-2 SV40 construct expressing c-myc tagged full length human receptor, were seeded into 96-well plates at a density of 3×10^5 cells per well in Hams F-12 medium (supplemented with 2 mmol/L glutamine, 10% fetal calf serum, 1 μg/mL puromycin). PAE-VEGFR-2 cells were grown for 24 hour at 37°C before starving for 2 hour with serum free medium. Antibodies were diluted in serum free medium then added to a final concentration

of 10 μg/mL and incubated for 1 hour at 37°C. The cells were then stimulated with VEGF-A ligand (Sigma-Aldrich), at a final concentration of 20 ng/mL, for 20 minutes at room temperature. Medium was aspirated and ice cold 70 μL lysis buffer (25 mmol/L Tris-HCl pH 6.8, 3 mmol/L EDTA pH 8, 3 mmol/L EGTA pH 8, 50 mmol/L sodium fluoride, 2 mmol/L sodium orthovanadate pH 10, 270 mmol/L sucrose, 10 mmol/L glycerophosphate, 10 mmol/L sodium pyrophosphate, 0.5% Triton X-100) added and incubated for a further 40 minutes at 4°C. After lysis was complete, 50 μL was transferred to an ELISA plate and left overnight at 4°C. ELISA plates (high protein binding capacity 96-well plates (Greiner Bio-One Limited) were coated overnight with 9B11 c-myc mouse mAb (Cell signaling Technology) at 1.25 μg/mL in PBS. Plates were blocked for 2 hours with 3% BSA/PBS and washed 3 times with PBS. To detect the captured phosphorylated receptor biotinylated 4G10 mAb (Millipore), diluted 1:2000 in 3% BSA/PBS, was added and incubated at room temperature for 1 hour, washed with PBS 3 times and then incubated for a further 1 hour with streptavidin conjugated HRP (GE Healthcare) diluted 1:16000 in 3% BSA/PBS. Each plate was finally washed 3 times with PBS and incubated with QuantaBlu substrate (Thermo Scientific) as per manufacturer's recommendations. The phospho VEGFR-2 signal was obtained by measuring light emitted at 465 nm after excitation at 340 nm using a Safire fluorescence plate reader (Tecan Group Ltd.). IC_{50} values were calculated by curve fitting with Origin 7.5 software (Origin Lab Corporation). HUVECs were plated in 24 well plates in MCDB131, 11 mmol/L L-glutamine, 2% FCS, and incubated overnight at 37°C, 5% CO_2. The following day the media was tipped off the cells and replaced with serum free media and serum starved for 2 hours 30 minutes at 37°C. Cells were incubated with blocking antibodies for 90 minutes at 37°C, and then stimulated with 50 ng/mL VEGF-A for 5 minutes. Media was then removed, cells washed and then lysed in radioimmunoprecipitation assay (RIPA) buffer, [RIPA—60 mmol/L Tris pH 7.4, 150 mmol/L NaCl, 1 mmol/L EDTA, 10× RIPA Detergent (10% NP40 + 2.5% deoxycholate) and phosphatase inhibitor cocktail 1 (Sigma P2850), 2 (Sigma), and protease inhibitor (Sigma)], the plates were sealed and left shaking at room temperature for 5 minutes. The lysates were snap frozen on dry ice and left overnight at −20°C. The DuoSet IC Human Phospho-VEGFR-2 (KDR) ELISA kit from R&D Systems was used to measure the levels of phospho-VEGFR-2 in the lysates. One hundred microliter of each lysate was used in the ELISA. The protocol as described in the manual was followed until the plate development stage where Supersignal West Pico Substrate (Pierce) was used. The plates were read by luminescence on a Tecan plate reader.

Two-dimensional tube formation assay

The effect of the VEGFR-2 antibodies on endothelial cell tube formation was measured using commercially available angiogenesis kits. Antibody titrations were prepared in MCDB 131 media containing 2% foetal calf serum and 11.6 mmol/L L-glutamine. The plates were incubated at 37°C, 5% CO_2 and treated with antibody as described in the manufacturers protocol so that on days 1, 4, 7, and 9 the media was removed and replaced with 0.5 mL of fresh antibody solution. Each antibody dilution or isotype control was tested in triplicate wells and the cultures were maintained at 37°C in 5% CO_2. Tubule formation was examined at day 11 following fixing and staining of tubules for CD31 using a tubule staining kit according to the manufacturers protocol (TCS Cell Works catalogue no. ZHA-1225). Briefly the media was removed from each well and the cells fixed for 30 minutes with 1 mL of 70% ethanol per well. The cells were incubated with 0.5 mL per well of 1 in 400 diluted mouse anti-CD31 antibody in PBS/1% BSA for 1 hour at 37°C, 5% CO_2. The cells were washed 3 times with PBS/1% BSA and then incubated with 0.5 mL per well of 1 in 500 diluted anti-mouse IgG alkaline phosphatase in PBS/1% BSA for 1 hour at 37°C, 5% CO_2. The cells were washed 3 times with distilled water and 0.5 ml per well of 5-bromo-4-chloro-3-indolyl phosphate/nitro blue tetrazolium (BCIP/NBT) solution added (1 tablet dissolved per 20 mL of water). The plates were incubated for 10 minutes at 37°C, 5% CO_2 and the stain was then washed off with 3 times distilled water, 1 ml per well. As a result of the anti-mouse IgG alkaline phosphatase activity the development of a dark purple color occurred in the location of CD31 expression in the HUVECs and reflected tubule formation. The color was allowed to develop over 10 minutes and the plates were subsequently washed with water and air dried. The development of a dark purple color within 10 minutes reflected tubule formation. Quantification of tubule growth was conducted by whole-well image analysis methodology using a Zeiss KS400 3.0 Image Analyser. The morphological parameters measured in the quantification methodology were total tubule length and number of branch points. All tubule formations within each of the 24 wells were measured excluding a rim of 100 μm depth to avoid edge retraction artifact. The inhibition of tube formation was plotted as percent inhibition of tube length or branch points compared to the isotype control.

Three-dimensional endothelial cell growth

The effect of the VEGFR-2 antibodies on endothelial cell tube formation within a 3D matrix was measured using a method adapted from that published (14). Rehydrated Cytodex 3 beads (~15,000) were coated with a 3:1 HUVEC: NHDF cell mix in 5 mL of endothelial cell basal medium 2 (EGM-2; Promocell) to give approximately 250 cells per bead. The bead cell mix was incubated at 37°C, 5% CO_2 for 4 hours with shaking every 30 minutes after which it was transferred to a T75 tissue culture flask and incubated overnight at 37°C, 5% CO_2 in a total volume of 20 mL EGM media. The following day the beads were dislodged from the flasks and transferred to

a 30 mL universal tube and allowed to settle. The coated beads were washed twice with EGM-2 allowing the beads to settle by gravity between washes. Fibrinogen (10 mg/mL) added to give a final concentration of 2 mg/mL and Aprotonin added to give a final concentration of 50 μg/mL. Meanwhile thrombin was diluted to 20 units per mL of EGM-2 and 10 μL pipetted per well into the middle 60 wells of a 96 well plate. The bead mix was gently swirled and poured into a reservoir. Keeping the reservoir rocking, 90 μL per well of the bead mix was pipetted into each well onto the thrombin. The fibrinogen/thrombin clot formed within 10 to 15 seconds and the plates were then placed at 37°C, 5% CO_2 for 15 minutes before dosing with antibody. Antibody titrations were prepared at 2 times the final assay concentration in EGM-2 containing 10 ng/mL VEGF-A to give a final assay concentration of 5 ng/mL VEGF-A. One hundred μL of each antibody dilution was pipetted into triplicate wells of the embedded beads. The plate was incubated for 8 days at 37°C, 5% CO_2. The media above the beads was carefully removed and the wells washed once with PBS. The cells were fixed by adding 50 μL per well of 3.7% formaldehyde plus 0.1% triton X-100 and incubating at room temperature for 1 hour. The formaldehyde solution was removed and each well washed 3 times with 200 μL per well of PBS. Following the final wash, 100 μL of PBS/1% BSA was added per well and the plates blocked for an hour at room temperature. The plates were washed 3 times with 200 μL per well of PBS/0.05% Tween and 100 μL per well of a solution of Hoecsht 33258 (diluted 1 in 500 in PBS/1% BSA) and anti-CD31-Alexa 488 (1 in 250 in PBS/1% BSA) added. The plates were incubated at room temperature for 1 hour. Excess anti-CD31-Alexa 488 and Hoecsht were washed out at room temperature over 2 days with 3 to 4 changes of 100 μL per well of PBS. The plates were imaged on the Cellomics Arrayscan.

Human endothelial cell Matrigel plug model

A human endothelial cell Matrigel plug model was carried out by ProQinase using the following method. The experiment was conducted in severe combined immunodeficient mice (SCID) mice. HUVEC spheroids were prepared as described earlier (15) by pipetting 100 HUVECs in a hanging drop on plastic dishes to allow overnight spheroid formation. The following day HUVEC spheroids were harvested and mixed in a Matrigel/fibrin solution with single HUVECs to reach a final number of 100,000 HUVECs as spheroids and 200,000 single HUVECs per injected plug. VEGF-A and fibroblast growth factor 2 (FGF-2) was added at a final concentration of 1000 ng/mL. Ten SCID mice per treatment group were subcutaneously injected with 500 μL of the cell/matrix suspension that quickly polymerized. Twice weekly dosing of the antibodies started the following day (day 1). On day 21 the study was terminated. The Matrigel plugs were removed, photographed and fixed in 4% Roti-Histofix (Roth) at room temperature for 4 to 12 hours. Thereafter the plugs were paraffin embedded using the semienclosed tissue processor Leica TP1020 with a standard procedure. For histological examination of the human vasculature, paraffin sections (thickness = 8–10 μm) were prepared from all plugs. Blood vessel formation and coverage by pericytes were detected by staining for human CD34 [green fluorescence (fluorescein isothiocyanate), NCL-END, Menarini] and smooth muscle actin (SMA; red fluorescence [Cy3]; Clone 1A4, Sigma). Three sections per plug were analyzed and 3 images were taken from each section at a magnification of 200× using the Eclipse TE2000-U microscope (Nikon). The area analyzed per section (3 images) was 0.44 mm^2. The vessel number (CD34 positive) was determined subtracting the highest peak in the histogram as constant background from the image. Thereafter red areas were detected above the threshold red (0:255), green (30:255), and blue (0:255) with an area diameter of 6.41. The detected area was separated using the function MorphoSeparateObjects(3.2). The resulting object count was used as vessel number. The number of CD34/α-SMA positive vessels was manually determined after vessel counting. The NIS-elements basic research software (Nikon) was used. Statistical significance was evaluated using the Mann-Whitney *U* test.

Human skin chimera model

EpiStem assessed the impact of 33C3 on normal vasculature using a human skin chimera model. Briefly, normal breast skin was obtained from 4 individual donors undergoing cosmetic surgical procedures. Skin pieces, 1 to 2 cm^2 were grafted into an incision wound on each of the SCID mice and then clipped. Two mice per skin donor were randomized into each group with a total of 8 mice per group. A piece of donor (not xenografted) control human skin and a piece of the excised mouse skin (from the donor acceptance site) were taken and formalin fixed for use as positive controls for immunohistochemistry. Clips were removed 7 to 10 days after grafting, when the wounds had scabbed over. Twice weekly treatment with the antibodies began 4 days post grafting. All animals were sacrificed 42 days post grafting and the grafts, together with adjacent mouse skin, excised and fixed in 4% formaldehyde in PBS (pH 7.4). Sections, 3 μm thick, were stained with mouse monoclonal human anti-CD31 antibody, clone JC70A (Dako; catalogue no. M0823), followed by anti-mouse HRP, revealed using diaminobenzidine and counterstained with thionine. The number and area of all labeled blood vessels were measured within the xenograft using an Olympus BX-61 microscope fitted with an Ariol MB-8 image analysis system. Statistical significance was evaluated using a 1-way ANOVA.

Immunohistochemistry and immunofluorescence for visualization purposes

FFPE tissues, sectioned at 4 μm onto slides, were dewaxed and rehydrated. Antigen retrieval was performed in a RHS-1 microwave vacuum processor (Milestone) at 110°C for 5 minutes in pH 9 retrieval buffer

(S2367, Dako). Blocking was done using an avidin-biotin kit (SP-2002, Vector Laboratories), 3% hydrogen peroxide and serum free protein block (X0909; Dako). Primary antibodies were diluted 1:500 in antibody diluent (S0809; Dako) and incubated with sections for 1 hour. Sections were incubated for 30 minutes with mouse Envision secondary (K4007, Dako) for CD31 (JC70A) and rabbit Envision secondary (K4003, Dako) for VEGFR-2 (55B11) and CD31 (CHG-CD31-P1), developed in diaminobenzidine for 10 minutes (K3466, Dako) and counterstained with Carazzi's hematoxylin. Appropriate no primary antibody and isotype controls were performed for each antibody. For immunofluorescence (IF), antigen retrieval was carried out as above, after blocking in 20% horse serum, sections were incubated for 1 hour with 55B11 and JC70A both at 1:20 in serum. Sections were incubated with donkey anti-rabbit IgG conjugated to Alexa Fluor 555 (A31572; Molecular Probes) and donkey anti-mouse IgG Alexa Fluor 488 (A21202) at 1:800 in serum for 30 minutes and counterstained with ProLong Gold antifade reagent with 4′,6-diamidino-2-phenylindole (DAPI; P36931; Molecular Probes). Fluorescent images were scanned and captured using a MIRAX scan (Carl Zeiss).

Results

33C3 binds VEGFR-2 domains 4-7

To generate fully human antibodies, XenoMouse was immunized with recombinant human receptor corresponding to ECDs 1-7. More than 1600 antibodies were identified using a combination of ELISA and FACS assays for binding to soluble recombinant human VEGFR-2 and HUVECs, respectively. The hits were then selected based on the ability to bind domains 4-7 of VEGFR-2 and functional inhibition of VEGF-A induced phosphorylation of VEGFR-2 in HUVEC. This yielded 627 antibodies able to bind to domains 4-7, of which 257 were also functional blockers. Thirty of this group were then selected for cloning and further analysis. Interestingly, despite the high hit rate in this screen, no antibodies were found that showed strong binding to mouse VEGFR-2 by ELISA. From 30 antibodies cloned, 12 independent lineages, as judged by sequence, were identified. These lineages were then progressed to further screening through a range of functional assays. This screening identified 33C3 as the antibody that fulfilled all the desired design characteristics.

The binding properties of 33C3 were further characterized using a number of binding and cross-competition assays. Binding to VEGFR-2 Ig domains 4-7 was confirmed by immobilizing 33C3, a VRLB domain targeting antibody, or IgG control on a plate and assessing the ability of each antibody to capture recombinant VEGFR-2 Ig domain 4-7 (Fig. 1A) or full length VEGFR-2 (Fig. 1B). Only 33C3 was able to capture VEGFR-2 Ig domains 4-7 (Fig. 1A), while both 33C3 and the VRLB antibody bound to the full length receptor (Fig. 1B). The experiment was also done in reverse with the VEGFR-2 Ig domains 4-7 immobilized, and the antibodies in solution (Fig. 1C). Consistent with the previous experiment only 33C3 bound the immobilized receptor confirming the interaction with Ig domains 4-7. To determine specificity of 33C3 a competition assay was used (Fig. 1D). Soluble recombinant proteins corresponding to full length VEGFR-1, murine VEGFR-2, Ig domains 4-7 of human VEGFR-2, and full length human VEGFR-2 were used to compete binding of 33C3 to immobilized full length VEGFR-2. Soluble ECDs corresponding to domains 4-7 and domains 1-7 competed with 33C3 for binding to immobilized VEGFR-2, confirming 33C3 binds full length VEGFR-2 in the dimerization domain (Fig. 1D). In contrast, soluble VEGFR-1 and murine VEGFR-2 did not compete for binding to immobilized human VEGFR-2 confirming previous observations that the antibodies were selective for VEGFR-2 and did not bind murine receptor. The affinity of 33C3 for recombinant VEGFR-2 as measured by BIAcore was less than 1 nmol/L (Fig. 1E).

The binding of 33C3 to VEGFR-2 expressed in PAE-VEGFR-2 cells was determined by FACS (Fig. 1F). 33C3 showed good binding to VEGFR-2 in the context of a cell showing the epitope was accessible. It showed similar binding to VEGFR-2 expressed on HUVECS (data not shown). To ensure that 33C3 binds an epitope distinct from the ligand binding site, PAE-VEGFR-2 cells were used to determine competition for binding between 33C3 and VRLB. The PAE-VEGFR-2 cells were preincubated with 33C3, VRLB and the relevant isotype controls, and then cell binding to plates coated with the VRLB antibody (Fig. 1G) and 33C3 (Fig. 1H) determined. 33C3 did not prevent cells binding to the VRLB antibody, while the VRLB antibody blocked binding to itself (Fig. 1G). Conversely, 33C3 competed binding of cells to itself, while the VRLB had only a small effect (Fig. 1H). The modest impact of VRLB antibody on binding to 33C3 may indicate some steric inhibition of the VRLB to 33C3, allosteric modulation of VEGFR-2, or some impact on the levels of VEGFR2. These data are consistent with 33C3 binding the Ig domains 4-7 of VEGFR-2.

Binding to VEGFR-2 Ig domains 4-7 inhibits VEGF-A mediated activation of VEGFR-2

To determine the functional properties of 33C3, the ability to block binding of VEGF-A to recombinant receptor and to inhibit VEGF-A mediated auto-phosphorylation of VEGFR-2 was tested. The VRLB antibody targeting the VEGF binding domain prevented binding of VEGF-A to VEGFR-2 overexpressed on PAE cells (Fig. 2A). In contrast, 33C3 had no effect on the binding of VEGF-A to VEGFR-2 (Fig. 2A) confirming 33C3 does not interfere with the interaction between VEGF-A and VEGFR-2. The ability of 33C3 to prevent VEGF-A mediated phosphorylation of VEGFR-2 was tested in the PAE-VEGFR-2 cells. Under these assay conditions, 33C3 is a potent inhibitor of VEGF-A induced phosphorylation of VEGFR-2 (Fig. 2B), inhibiting receptor phosphorylation with a mean IC_{50} of

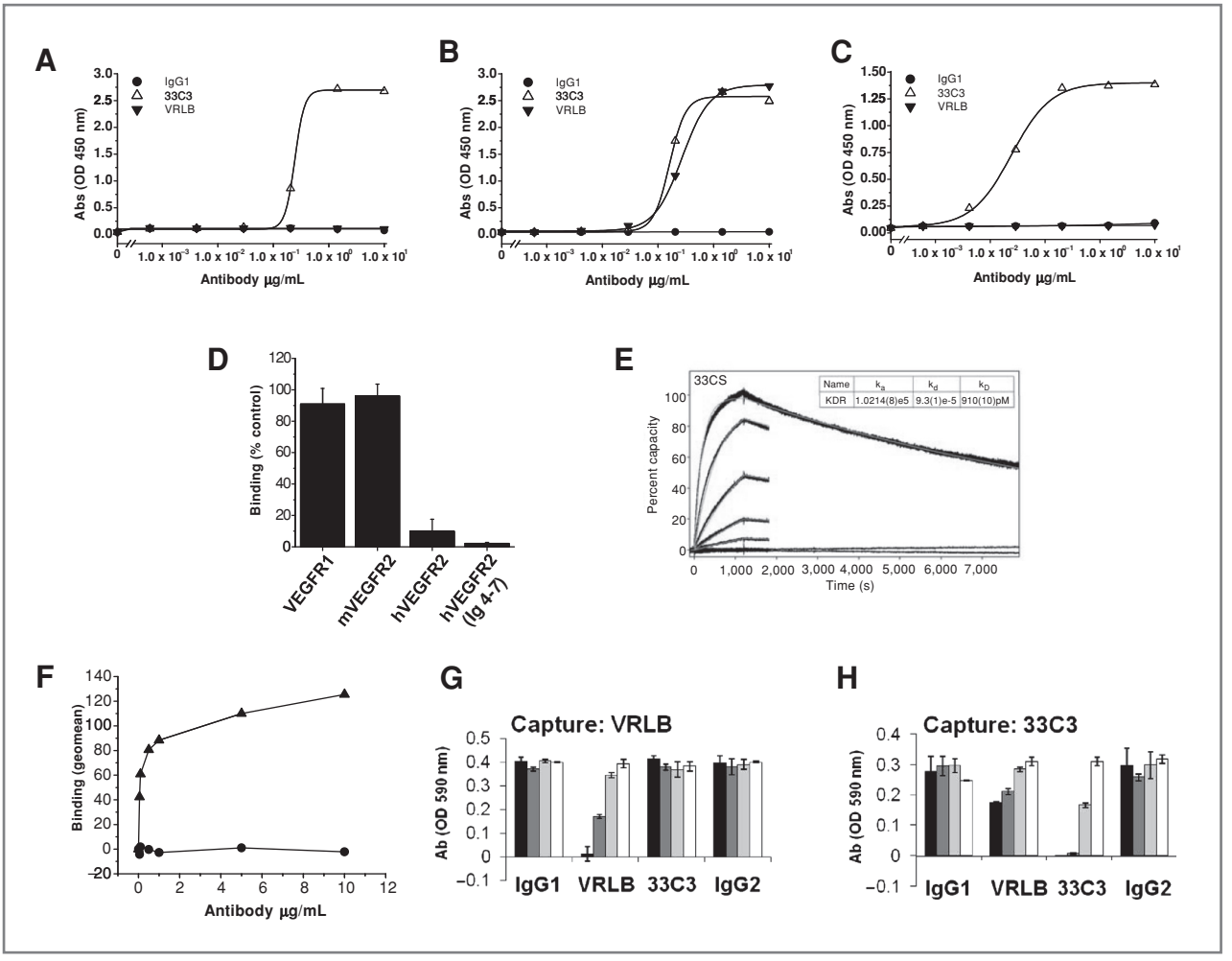

Figure 1. 33C3 specifically binds VEGFR-2 by interacting with Ig domains 4-7. To confirm that 33C3 binds to Ig domains 4-7 of VEGFR-2, IgG control, 33C3, or VRLB were immobilized on plates at the range concentrations indicated and incubated with either soluble VEGFR-2 (domains 4-7; A) or VEGFR-2 (domains 1-7; B) at 20 μg/mL. Bound protein was detected using anti-his HRP and TMB reagent. In addition, VEGFR-2 Ig domains 4-7 at 10μg/mL were coated on a plate and incubated with IgG control, 33C3, or VRLB at the concentrations indicated. C, binding of the antibody detected with anti-human IgG HRP and TMB reagent. (A, B, and C are representative of 2 identical experiments). D, specificity for human VEGFR-2 was determined using a cross-competition assay. Full length VEGFR-2 was immobilized on the plate and 0.1μg/mL 33C3 allowed to bind in the presence of recombinant VEGFR-1, murine VEGFR-2 (mVEGFR-2), human VEGFR-2 (domains 1-7; hVEGFR-2) at 5 μg/mL, and human VEGFR-2 (domains 4–7; hVEGFR-2 Ig 4–7) at 25 μg/mL. Representative of the mean of 2 identical experiments. E, affinity of 33C3 for full length recombinant VEGFR-2 was determined by BIAcore. F, binding of 33C3 to PAE-VEGFR-2 cells was determined by FACS. 33C3 was incubated with PAE-VEGFR-2 cells at the concentrations indicated for 1 hour at 4°C, and binding was detected by staining with anti-human IgG Alexa 488 (▲, 33C3; ●, IgG) . To confirm 33C3 does not bind near the ligand binding site in the context of VEGFR-2 expressed on PAE-VEGFR-2 cells, the ability of 33C3 to compete with a VRLB antibody was determined. VRLB (G) and 33C3 (H) antibodies were coated on the plate and cells incubated in the presence of 10 (black bars), 1 (dark gray bars), 0.1 (light gray bars), and 0.01 (open bars) μg/mL IgG1 control, VRLB, 33C3, or IgG2 control for 1 hour at 4°C. Bound cells were detected by crystal violet staining. Representative of 3 identical experiments.

99 ± 3 μg/mL. The ability of 33C3 to block VEGF-A stimulated phosphorylation in HUVECs was tested (Fig. 2C), together with the VRLB blocking antibody (Fig. 2D). Both the 33C3 antibody and the VRLB antibody were equally effective at preventing activation of VEGFR-2. Theoretically it is possible that an antibody targeting the Ig 4-7 domains of VEGFR-2 would have some form of agonist activity. Lack of agonism was set as a critical design goal, and consistent with this, 33C3 showed no agonist properties in the absence of ligand (data not shown). These data establish that targeting the Ig 4-7 domains of VEGFR-2 produces an antibody that inhibits the activation of the receptor, without interfering with the interaction of the ligand.

33C3 inhibits endothelial tube formation *in vitro*

Aspects of the angiogenic process dependent on VEGFR mediated signaling can be modeled using *in vitro* endothelial–fibroblast coculture assays. The ability of 33C3 to inhibit VEGF-A dependent angiogenic processes was determined using 2 different assay systems. The first was a 2-dimensional fibroblast–endothelial coculture

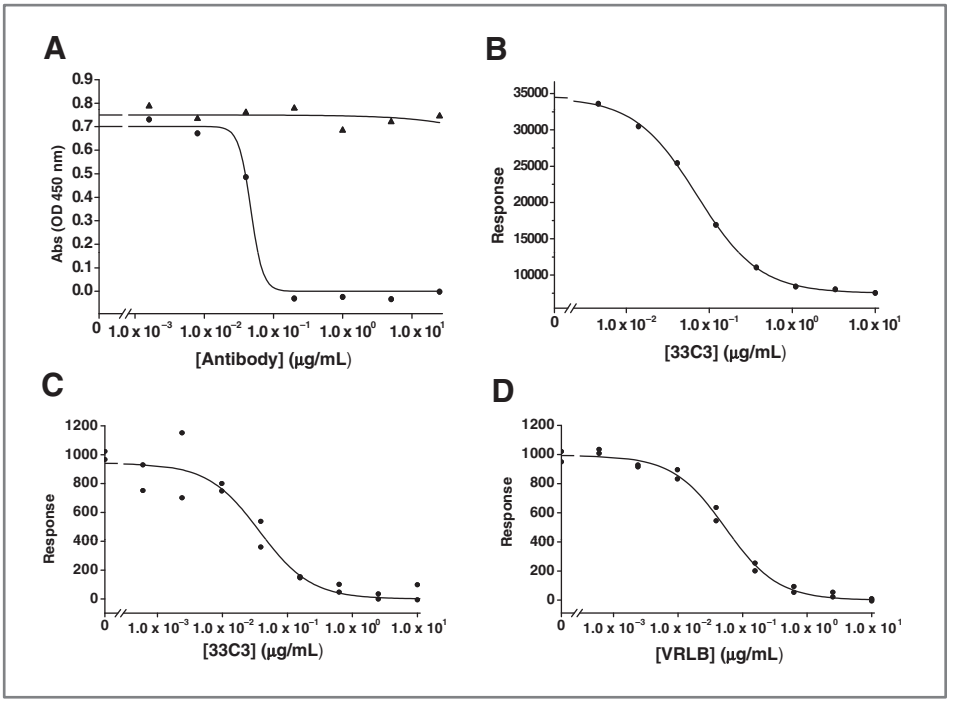

Figure 2. 33C3 inhibits VEGFR-2 activation but not ligand binding. A, the ability of 33C3 (▲) and VRLB antibody (●) to inhibit VEGF-A binding to recombinant VEGFR-2 was assessed using a solid phase binding assay. VEGF-A was immobilized in a 96-well plate and recombinant VEGFR-2 allowed to bind in the presence of 33C3 and VRLB at the concentrations indicated. Bound VEGFR-2 was detected with a polyhistidine-HRP conjugated antibody. Representative of at least 2 identical experiments. B, the potency of 33C3 was determined using PAE-VEGFR-2 cells stimulated with 50 ng/mL VEGF-A for 5 minutes. VEGFR-2 was captured from cell lysates using an antibody recognizing the His-tag and the amount of phosphorylated receptor detected with an anti-phosphotyrosine antibody. The cellular potency of 33C3 (C) and VRLB (D) antibodies were compared in HUVEC cells stimulated with VEGF-A. Serum-starved HUVECs were preincubated with antibodies before stimulation for 5 minutes with 50 ng/mL VEGF-A. The level of phosphorylated VEGFR-2 was determined using a VEGFR-2 phospho-ELISA. Representative of 3 identical experiments.

assay that we have previously shown to be sensitive to VEGFR inhibition (4,16). 33C3 gave a dose dependent inhibition of tube formation with a mean EC_{50} of 25 ng/mL for tube length (Fig. 3A). Consistent with the reduction in tube length the number of bifurcations or branch point were inhibited with an IC_{50} of 19 ng/mL. Maximal inhibition was seen at approximately 2 μg/mL, where only residual endothelial pools or very short tubes remain (Fig. 3A and D). The ability to reduce tube formation was similar to that of the VRLB antibody (Fig. 3B and E), and also small molecule VEGFR TKIs (data not shown; ref. 4). Isotype controls have no impact on tube formation in this assay [Fig. 3C (i and ii)], nor did 33C3 have any effect on the fibroblast monolayer. The effect of 33C3 in this assay mimics the observations made for other classical inhibitors of VEGF signaling in this assay format. A second assay commonly used to study angiogenic processes *in vitro* is a 3D tubule outgrowth assay (17, 18). Endothelial tube formation is driven differently in this assay compared to the 2D tube formation. In the 2D assay, tubes form on top of the fibroblast monolayer, while in the 3D assay endothelial cells coated on the beads migrate or proliferate to form tubes within the matrix. Therefore, to further validate the utility of 33C3 as a VEGFR-2 antagonist, the ability to inhibit tube formation in this assay format was tested (Fig. 4). This assay was modified from published methods such that fibroblasts and endothelial cells were coseeded on beads prior to suspension in a collagen matrix, rather than have a fibroblast feeder layer. In this format of the assay, fibroblasts migrate rapidly away from the bead and distribute through the gel. After 5 days, endothelial tube formation is evident in the control wells (Fig. 4E) with 33C3 giving a dose dependent reduction in tubule outgrowth (Fig. 4A to D). Although the endothelial cells remained associated with the beads and failed to form tubes, 33C3 had no impact on the fibroblasts which migrated away from the beads suggesting its effects were specific for endothelial cells. Collectively these data show that 33C3 is an effective inhibitor of VEGFR dependent phenotypes *in vitro*, and are consistent with it being an effective inhibitor of VEGF-A induced signaling.

Targeting VEGFR-2 Ig 4-7 domains effectively suppresses angiogenesis *in vivo*

Having established that 33C3 is effective at preventing activation of VEGFR-2 *in vitro*, we next assessed whether this mode of action was able to block angiogenesis *in vivo*. Given 33C3 does not cross-react with murine VEGFR-2, and because we were unable to generate viable transgenic

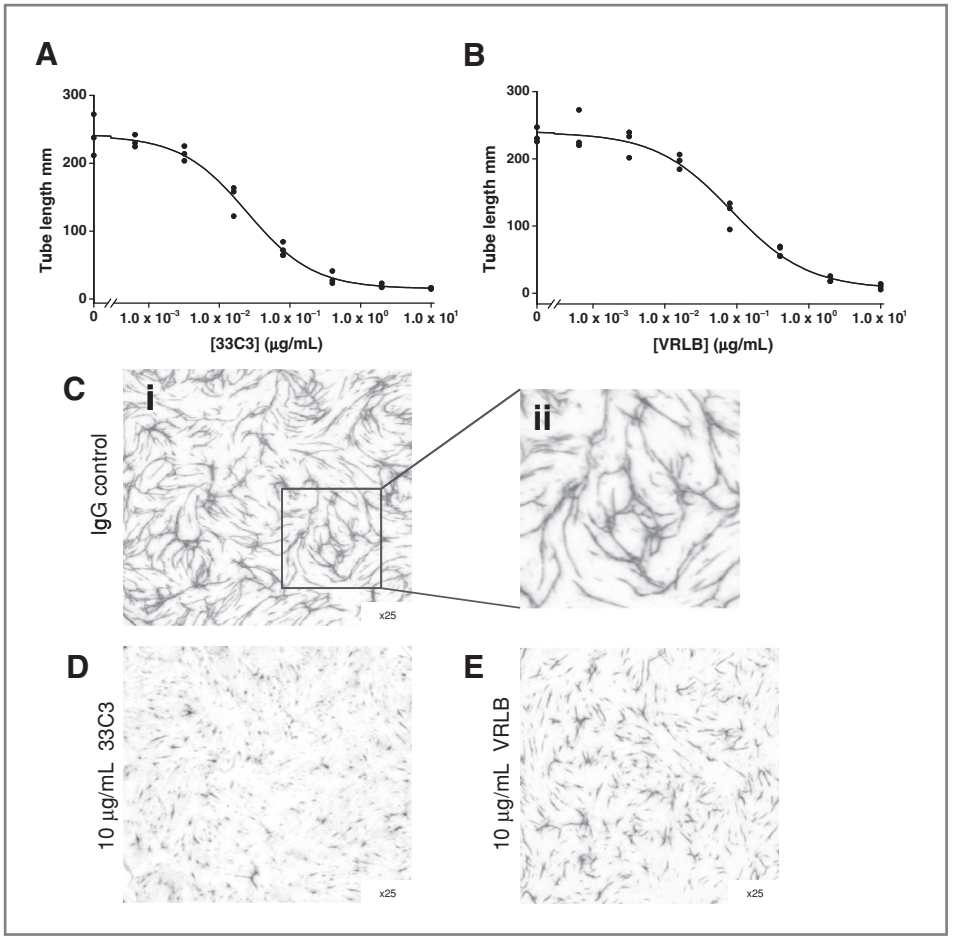

Figure 3. 33C3 inhibits endothelial tube formation in a 2D coculture model. 33C3 (A, D) and VRLB (B, E) antibodies, together with their relevant IgG controls (C), were were tested for the ability to inhibit endothelial tube formation in a fibroblast–endothelial coculture system. 33C3, VRLB, and control IgG antibodies were incubated at a range of concentrations for 11 days, and tube formation was visualized by staining HUVEC cells with a CD31 antibody. Tube length measured in mm was quantified by image analysis. Dose response curves are shown for 33C3 (A) and VRLB (B). Representative images are shown for IgG controls (C, i and ii), 33C3 (D), and VRLB (E). Images are captured at ×25 magnification. Data is representative of more than 3 identical experiments.

mice expressing human VEGFR-2, we used 2 murine preclinical models that allow the action of therapeutics on functional human blood vessels to be modeled.

We first tested the efficacy of 33C3 in a human endothelial cell Matrigel plug model. Human endothelial cells seeded into Matrigel containing FGF-2 and VEGF-A are implanted into SCID mice. Over time the human endothelial cells form fully functional vessels comprised of human endothelial cells that are fused with mouse vessels that invade the plug (15). When administered at 1 mg/kg twice weekly, 33C3 was able to reduce the level of human vessels by more than 70% (3 separate experiments) as measured by CD34 staining. In a single experiment comparing 33C3 with the VRLB antibody (1 mg/kg), 33C3 was almost as effective as the VRLB antibody at inhibiting angiogenesis in this model (Fig. 5A and C). Not all human vessels were ablated by either VEGFR-2 antibody (Fig. 5A and C). In every experiment a small number of large vessels remain. Whether these represent vessels that are formed by a mechanism independent of VEGFR-2 signaling, or angiogenic vessels resistant to VEGFR-2 inhibition, is not clear. Although the numbers of human vessels were significantly reduced, neither 33C3 nor VRLB antibody changed the ratio of smooth SMA positive vessels within the plug (Fig. 5B). The effects on the human vessels are specific to 33C3 and VRLB antibody as isotype matched control antibodies have no effect on vessel number in this model, even when dosed at 10 mg/kg twice weekly (Fig. 5A and C). More work would be required to determine whether the slightly greater but nonsignificant impact of VRLB over 33C3 in this model is a meaningful difference that may differentiate the mode of action of the 2 antibodies in terms of efficacy or toxicity.

The second model used was a human skin chimera model. Human skin is transplanted on to the back of SCID animals, and over a period of weeks the established human vessels within the skin graft become perfused again by fusing with murine vessels (Fig. 6A). The established human skin graft becomes well vascularized as shown by staining with a pan CD31 molecule (Fig. 6B). A significant proportion of the vessels in each graft are human as shown by staining with a human specific CD31 antibody (Fig. 6C). This is an attractive but challenging model in which to test therapeutics as it provides the opportunity to assess the effects on real human vessels in the context of a human tissue. The human vessels within the graft are in an angiogenic state, staining positive for

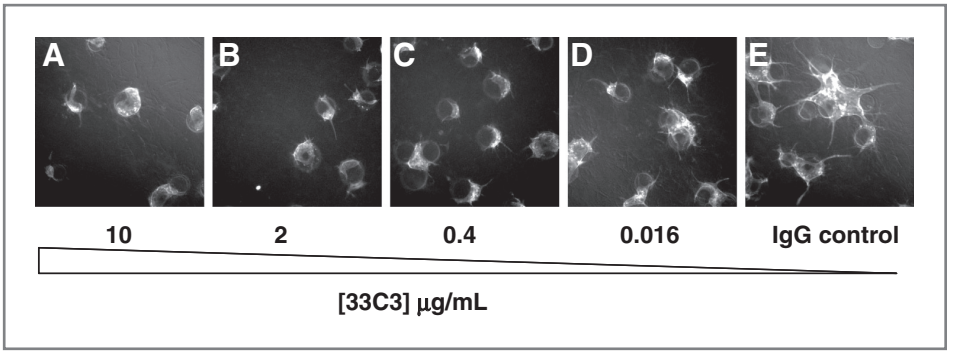

Figure 4. 33C3 inhibits endothelial tubule outgrowth in a 3D outgrowth assay. 33C3 was tested for the ability to reduce tubule formation in a 3D outgrowth assay. Beads coated in endothelial cells and fibroblasts were suspended in Matrigel in the presence of 5 ng/mL VEGF-A. 33C3 was used at 10 μg/mL (A), 2 μg/mL (B), 0.4 μg/mL (C), and 0.016 μg/mL (D). Isotype control antibody was used at 10 μg/ml (E). Endothelial tubes were visualized by staining with CD31-Alexa tagged antibody (A–E). Plates were imaged on a Cellomics Arrayscan. Images are captured at ×25 magnification. Data is representative of at least 3 identical experiments.

VEGFR-2 (Fig. 6D and E). We have previously established using small molecule VEGFR2 TKIs and the VRLB antibody that the human vessels were dependent on VEGFR-2 signaling (Kendrew and Barry, unpublished data). Using the same protocol we tested 33C3, specifically, 33C3 was dosed to animals with established human grafts from 4 individual donors for 38 days at 1 mg/kg. 33C3 specifically reduced the content of human vessels in the graft as determined by CD31 staining reducing both the number of vessels (Fig. 6F) and the vessel area (Fig. 6G). In this model, 33C3 was as effective as the VRLB antibody at reducing human angiogenic vessels within the skin graft. These effects are specific to the VEGFR-2 target blocking antibodies, as an irrelevant IgG control antibody tested in an independent set of skin grafts, had no effect vessel density (Fig. 6H) versus the vehicle only control group. The results in this experiment for the VRLB antibody were comparable to the pilot experiment. Collectively these data show that an antibody targeting VEGFR-2 Ig domains 4-7 is extremely effective at inhibiting angiogenesis of human vessels undergoing angiogenesis *in vivo*.

Discussion

We have identified a fully human therapeutic antibody 33C3 that inhibits VEGFR-2 activation by targeting the Ig domains 4-7 of VEGFR-2. Using a number of assays that model different aspects of the angiogenic process we show that this novel mode of action is as effective as other VEGF signaling inhibitors such as antibodies that inhibit receptor–ligand interaction and small molecular weight TKIs. 33C3 behaved consistently in all *in vitro* assays with a profile equivalent to that of a classic VEGFR inhibitor. It fully suppressed VEGF-A mediated activation of VEGFR-2, and downstream effects. In 2 different endothelial tubule formation assays, it gave full inhibition, indistinguishable from a ligand blocking antibody and TKIs. 33C3 delivers these effects by specifically targeting the Ig domains 4-7, and does not interfere with the ligand binding site of the receptor. Consistent with this it does not cross-compete with an antibody that blocks VEGF-A binding, or prevent binding of VEGF-A to recombinant VEGFR-2.

The failure to identify murine cross-reactive antibodies in the screen limited the number of models with which *in vivo* proof of principle could be shown. The effects of blocking VEGFR-2 with antibodies that target mouse receptor have been assessed with the ligand blocking antibody DC101. This antibody reduces angiogenesis and tumor growth in a number of models (19). Because we did not have a murine surrogate of 33C3, to model the effects of 33C3, we used the human Matrigel and human skin chimera models as an alternate approach to deliver *in vivo* proof of principle. These models recapitulate different aspects of angiogenesis. In the Matrigel plug assay individual endothelial cells coalesce to form new angiogenic vessels. The model is driven by specific ligands VEGF and FGF, but does not really assess the effects on remodeling of established or more mature vessels. 33C3 was extremely effective at preventing angiogenesis, significantly reducing the vessel number. However, in this model there were a small number of human vessels supported by cells staining strongly positive for SMA that were not targeted by 33C3. The recruitment of these cells to vessels is dependent on PDGFR signaling, which enhances tumor angiogenesis by recruiting pericyte and stromal fibroblasts to tumor vessels. Targeting these fibroblasts with PDGFR inhibitors in combination with VEGFR inhibition reduces vessel associated pericytes and myofibroblast resulting in an enhanced reduction in tumor angiogenesis and tumor growth (20–23). These SMA positive vessels may therefore represent mature vessels resistant to inhibition of VEGFR signaling or specifically resistant to 33C3. It would be interesting to determine whether these residual vessels are ablated when inhibition of VEGFR signaling is

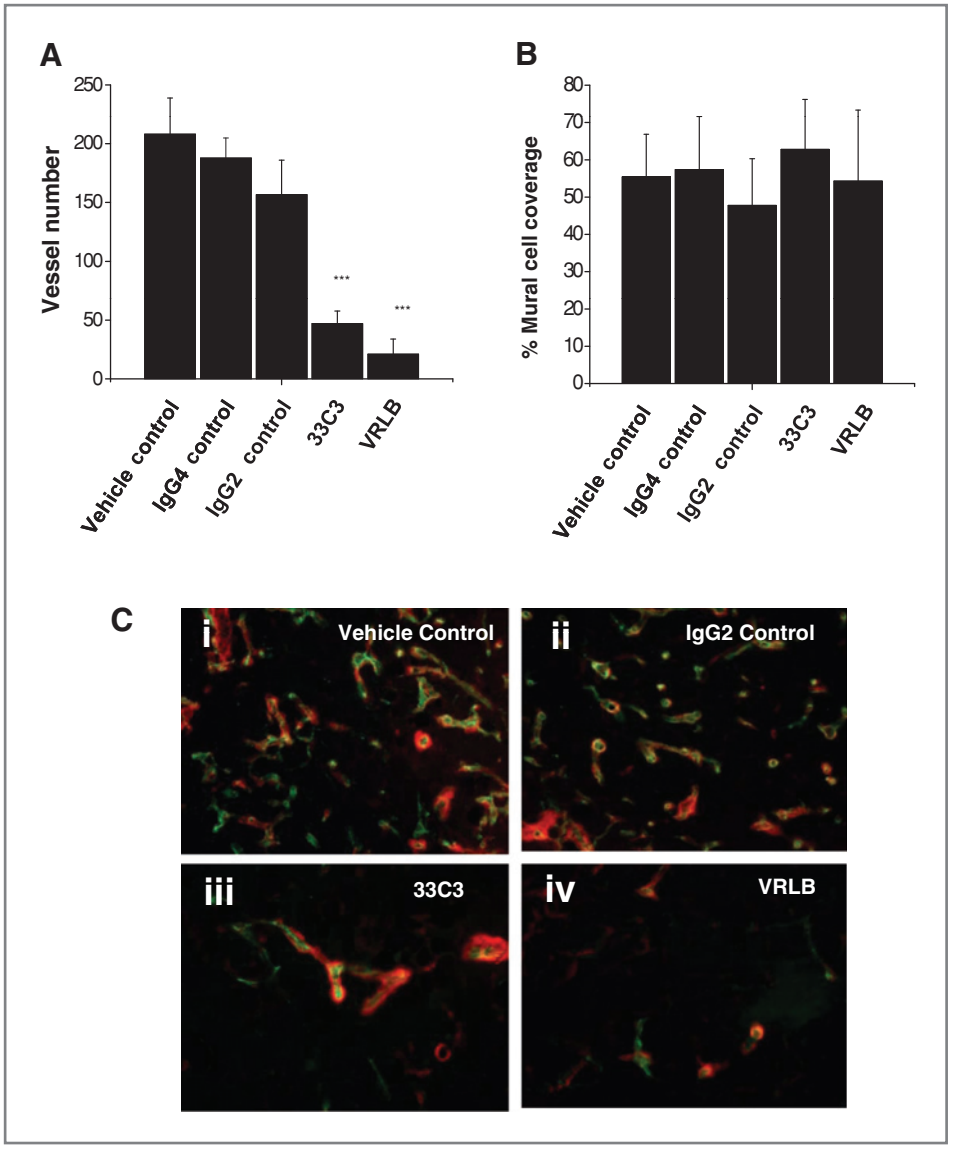

Figure 5. 33C3 reduces angiogenesis in a human Matrigel plug model. To determine whether 33C3 inhibits VEGFR-2 dependent angiogenesis, efficacy was tested in a Matrigel plug model in which human endothelial cells form human vessels in the presence of VEGF-A. Matrigel containing human endothelial cells, FGF-2, and VEGF-A was implanted into the flanks of SCID mice. Animals were dosed every 3 days with vehicle (PBS), 33C3 (1 mg/kg), VRLB (1 mg/kg), and IgG2 and IgG4 isotype controls (20 mg/kg). After 21 days, plugs were excised and stained for human vessels using a CD34 antibody (green) and for mural cells or fibroblasts using an antibody to SMA (red). A, the number of human vessels in each plug were counted, and the mean vessel number (±SEM) is represented. B, the mean percentage (±SEM) of mural cell positive vessels is represented. C, representative images of CD34 positive vessels (green) and SMA positive cells (red) are shown for vehicle (C, i), IgG2 (C, ii), 33C3 (C, iii), and VRLB (C, iv) treated plugs. ***, $P < 0.001$. Mann–Whitney *U* test.

combined with a PDGFR signaling inhibitor, or agents targeting these SMA positive cells.

The human skin chimera model is very different from the Matrigel plug model. The skin graft already contains established human vessels which become angiogenic as a result of the transplantation process. Moreover the angiogenic microenvironment of the graft is additionally invaded by murine vessels. Within an individual experiment, skin grafts from 4 individual donors are assessed in each treatment group. Hence each treatment group represents 4 independent tests. In this model, 33C3 effectively targeted the human vessels. It was able to prune angiogenic vessels as well as prevent the formation of nascent vessels, but did not have any effect on the murine vessels. It is possible that effects in models such as these can result from antibody dependent immune cell effects. In experiments where irrelevant isotype control antibodies have been tested, these had no effect on human vessels in the graft, when compared to the vehicle dosed control group. Likewise irrelevant isotype control antibodies had no significant effect on the vessel density in the human Matrigel model.

In an attempt to model the effect of 33C3 in preclinical efficacy models transgenic animals in which murine VEGFR-2 was replaced with the human VEGFR-2 receptor were generated. Although germline transmission was confirmed and animals heterozygous for the human receptor were generated, no homozygous animals were generated as the human receptor in these animals was nonfunctional. This was confirmed by assessing rises in VEGF stimulated by inhibition of VEGFR-2, a pharmacodynamic biomarker of VEGFR-2 inhibition (24–27).

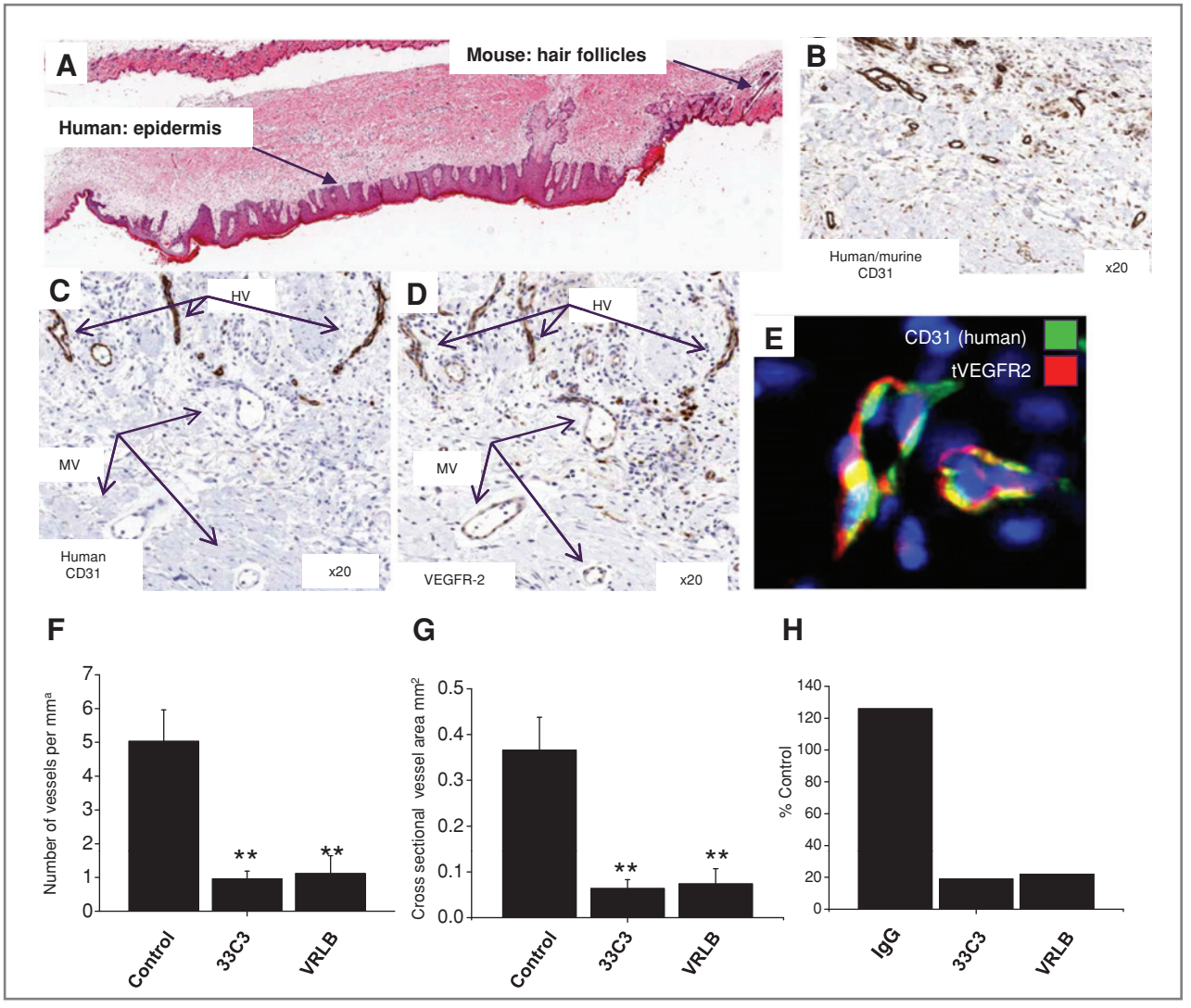

Figure 6. Inhibition of angiogenesis in a human skin chimera model. The ability of 33C3 and VRLB to reduce angiogenic vessels in human skin was determined using a human skin engraftment model. Animals bearing grafts were treated with PBS control, 33C3 (1 mg/kg every 3 days), and VRLB antibody (1 mg/kg every 3 days). A, a representative hematoxylin and eosin image of a whole graft is shown with the human epidermis and mouse epidermis indicated. B, the presence of human and murine vessels was determined by staining with a pan-CD31 antibody. Human vessels were stained with a human specific CD31 antibody (C and E) and in the next section, vessels were stained with a VEGFR-2 antibody (D). Human vessels (HV) and murine vessels (MV) are indicated with arrows. Human vessels were costained for with a human specific CD31 antibody (green) and a murine/human cross-reactive VEGFR-2 antibody (red; E). The human vasculature was quantified by image analysis (F, G, H). Mean human vessel density (±SEM) and the mean cross-sectional area (±SEM) are shown in F and G, respectively. The vessel number relative to the vehicle dosed control expressed as a percentage for an irrelevant IgG (from a separate set of grafts), 33C3, and VRLB antibody are shown (H) to show that treatment with IgG does not give a nonspecific effect on human vessels. **, $P < 0.01$. One-way ANOVA.

Treating heterozygous hVEGFR-2 expressing animals with DC101, resulted in an increase in circulating VEGF-A while treating with antibody targeting human VEGFR-2 did not elicit a biomarker response (i.e., a rise in VEGF-A; Kendrew and Barry, unpublished). Although we have been unable to generate data in classical tumor efficacy models the observations in the skin chimera model give confidence that 33C3 would have effects on established human vessels in a largely human microenvironment. That 33C3 and the VRLB antibody gave comparable results in both models further builds confidence that 33C3 has potential to deliver effects as a therapeutic molecule.

An antibody with the mode of action of 33C3 is an attractive way to inhibit the VEGFR-2 axis for a number of reasons. Inhibition of receptor activation would be specific for signals driven through VEGFR-2, contrasting with the more selective small molecule VEGFR TKIs which have additional pharmacologies within and beyond the VEGFRs (28). Moreover the molecule could

function independently of ligand concentration. VEGF ligands rise on treatment with various VEGF signaling inhibitors (24–27). Therefore on chronic dosing the efficacy of ligand sequestering antibodies, small molecular weight TKIs, and VEGFR ligand blocking antibodies, could be affected by high local VEGF concentrations. In addition both VEGFR-2 and VEGFR-1 are also expressed as soluble ECDs which serve to regulate the free levels of VEGF-A and other VEGF family ligands locally, modulating the physiological effects of VEGF-A and maintaining appropriate free levels of ligand. Ligand sequestrating agents, or receptor–ligand blockers, disrupt this sensitive secondary regulatory mechanism, impacting the circulating and local levels of free VEGF family ligands. For example a ligand blocking antibody could displace VEGF-A from soluble VEGFR-2. Large rises in free ligand have the potential to act as a resistance mechanism, ultimately competing with receptor for antibody, or swamping the ability of an antibody to suppress ligand. An agent with the mode of action of 33C3 would not be expected to have these secondary effects or be inhibited by rising VEGF concentrations. We have tried to address whether there are concentration dependent differences using the *in vitro* tube formation and pharmacology assays. Although we have seen some indication that the concentration of VEGF-A may not influence the efficacy of 33C3 the dynamic range in these assays is not sufficient to generate robust, statistically significant data sets (data not shown). Specifically the effective VEGF-A concentration range is limited between 1 and 30 ng/mL, with little stimulation seen below 1 ng/mL. Further work using *in vivo* efficacy models would be required to test this hypothesis robustly.

Targeting the dimerization domain to inhibit receptor activation offers opportunities to drive increased efficacy by combining with other VEGFR signaling inhibitors. Combining 2 different agents against the same receptor can result in more comprehensive suppression of a pathway. For example targeting erb2 signaling with a dimerization inhibiting antibody pertuzimab (2C4; 29, 30) delivers increased efficacy when used in combination with the herceptin (31). VEGFR also form homo- and heterodimers, which drives a complex series of signaling events leading to activation of many common growth factor signaling pathways (1). VEGFR-1 for example can synergize with VEGFR-2 and facilitate full activation of VEGFR-2 signaling (32, 33), and VEGFR-3 also forms a heterodimer (34). Formation of these heterodimers would be prevented by an inhibitor of VEGFR-2 dimerization. Although we have not been able to formally show inhibition of VEGFR-2 dimerization with 33C3 we would suggest that this is the most likely mode of action. Structural studies have confirmed that VEGF interacts with Ig domains 2 and 3 (35), while the Ig domain 7 is critical for driving dimer formation (36), with additional contributions from Ig domains 4 (35, 36). It is therefore reasonable to conclude that targeting the Ig domains 4-7 of VEGFR-2 would prevent receptor dimerizations. While this manuscript was being revised a paper describing an antibody 2E11 targeting VEGFR-3 Ig domain 5 was published (37). This antibody has similar properties to 33C3 albeit targeting the structurally related receptor VEGFR-3. Importantly 2E11 reduced the formation of VEGFR-3/VEGFR-2 heterodimers induced by VEGF-C. The observations in this paper therefore further support the hypothesis that an antibody targeting Ig domains 4-7 would inhibit receptor dimerization.

In summary, we have described a novel antibody, 33C3, with a new mode of action to target VEGFR-2 mediated signaling, and have shown that inhibition of VEGFR2 dimerization is an effective mechanism for inhibiting VEGFR mediated effects both *in vitro* and *in vivo*.

Disclosure of Potential Conflicts of Interest

No potential conflicts of interest were disclosed.

Acknowledgments

The authors thank Claire Barnes and Andrew Cassidy for help with VEGFR pharmacology assays, Graham Sproat and Ian Harden for expressing VEGFR-2 Ig domains 4-7, MedImmune Hayward for BIAcore analysis, ProQinase GMBH for collaborating on development of the human Matrigel plug assay, and Epistem for the human skin graft model.

The costs of publication of this article were defrayed in part by the payment of page charges. This article must therefore be hereby marked *advertisement* in accordance with 18 U.S.C. Section 1734 solely to indicate this fact.

Received September 17, 2010; revised January 17, 2011; accepted February 23, 2011; published OnlineFirst March 9, 2011.

References

1. Olsson AK, Dimberg A, Kreuger J, Claesson-Welsh L. VEGF receptor signaling—in control of vascular function. Nat Rev Mol Cell Biol 2006;7:359–71.
2. Kim KJ, Li B, Winer J, Armanini M, Gillett N, Phillips HS, et al. Inhibition of vascular endothelial growth factor-induced angiogenesis suppresses tumour growth *in vivo*. Nature 1993;362:841–44.
3. Holash J, Davis S, Papadopoulos N, Croll SD, Ho L, Russell M, et al. VEGF-Trap: a VEGF blocker with potent antitumor effects. Proc Natl Acad Sci U S A 2002;99:11393–98.
4. Wedge SR, Kendrew J, Hennequin LF, Valentine PJ, Barry ST, Brave SR, et al. AZD2171: a highly potent, orally bioavailable, vascular endothelial growth factor receptor-2 tyrosine kinase inhibitor for the treatment of cancer. Cancer Res 2005;65:4389–400.
5. Wedge SR, Ogilvie DJ, Dukes M, Kendrew J, Chester R, Jackson JA, et al. ZD6474 inhibits vascular endothelial growth factor signaling, angiogenesis, and tumor growth following oral administration. Cancer Res 2002;62:4645–55.
6. Wood JM, Bold G, Buchdunger E, Cozens R, Ferrari S, Frei J, et al. PTK787/ZK 222584, a novel and potent inhibitor of vascular endothelial growth factor receptor tyrosine kinases, impairs vascular endothelial growth factor-induced responses and tumor growth after oral administration. Cancer Res 2000;60:2178–89.
7. Mendel DB, Laird AD, Xin X, Louie SG, Christensen JG, Li G, et al. *In vivo* antitumor activity of SU11248, a novel tyrosine kinase inhibitor targeting vascular endothelial growth factor and platelet-derived growth factor receptors: determination of a pharmacoki-

netic/pharmacodynamic relationship. Clin Cancer Res 2003;9:327–37.
8. Wilhelm SM, Carter C, Tang L, Wilkie D, McNabola A, Rong H, et al. BAY 43–9006 exhibits broad spectrum oral antitumor activity and targets the RAF/MEK/ERK pathway and receptor tyrosine kinases involved in tumor progression and angiogenesis. Cancer Res 2004;64:7099–109.
9. Krupitskaya Y, Wakelee HA. Ramucirumab, a fully human mAb to the transmembrane signaling tyrosine kinase VEGFR-2 for the potential treatment of cancer. Curr Opin Investig Drugs 2009;10:597–605.
10. Lu D, Shen J, Vil MD, Zhang H, Jimenez X, Bohlen P, et al. Tailoring *in vitro* selection for a picomolar affinity human antibody directed against vascular endothelial growth factor receptor 2 for enhanced neutralizing activity. J Biol Chem 2003;278:43496–507.
11. Christinger HW, Fuh G, de Vos AM, Wiesmann C. The crystal structure of placental growth factor in complex with domain 2 of vascular endothelial growth factor receptor-1. J Biol Chem 2004;279:10382–388.
12. Fuh G, Li B, Crowley C, Cunningham B, Wells JA. Requirements for binding and signaling of the kinase domain receptor for vascular endothelial growth factor. J Biol Chem 1998;273:11197–204.
13. Kearney JF, Radbruch A, Liesegang B, Rajewsky K. A new mouse myeloma cell line that has lost immunoglobulin expression but permits the construction of antibody-secreting hybrid cell lines. J Immunol 1979;123:1548–50.
14. Nakatsu MN, Davis J, Hughes CC. Optimized fibrin gel bead assay for the study of angiogenesis. J Vis Exp 2007;3:186–7.
15. Korff T, Augustin HG. Integration of endothelial cells in multicellular spheroids prevents apoptosis and induces differentiation. J Cell Biol 1998;143:1341–52.
16. Brave SR, Eberlein C, Shibuya M, Wedge SR. Barry ST. Placental growth factor neutralising antibodies give limited anti-angiogenic effects in an *in vitro* organotypic angiogenesis model. Angiogenesis 2010;13:337–47.
17. Pan Q, Chanthery Y, Liang WC, Stawicki S, Mak J, Rathore N, et al. Blocking neuropilin-1 function has an additive effect with anti-VEGF to inhibit tumor growth. Cancer Cell 2007;11:53–67.
18. Pan Q, Chathery Y, Wu Y, Rathore N, Tong RK, Peale F, et al. Neuropilin-1 binds to VEGF121 and regulates endothelial cell migration and sprouting. J Biol Chem 2007;282:24049–56.
19. Prewett M, Huber J, Li Y, Santiago A, O'Connor W, King K, et al. Antivascular endothelial growth factor receptor (fetal liver kinase 1) monoclonal antibody inhibits tumor angiogenesis and growth of several mouse and human tumors. Cancer Res 1999;59:5209–18.
20. Bergers G, Song S, Meyer-Morse N, Bergsland E, Hanahan D. Benefits of targeting both pericytes and endothelial cells in the tumor vasculature with kinase inhibitors. J Clin Invest 2003;111:1287–95.
21. Erber R, Thurnher A, Katsen AD, Groth G, Kerger H, Hammes HP, et al. Combined inhibition of VEGF and PDGF signaling enforces tumor vessel regression by interfering with pericyte-mediated endothelial cell survival mechanisms. FASEB J 2004;18:338–40.
22. Anderberg C, Li H, Fredriksson L, Andrae J, Betsholtz C, Li X, et al. Paracrine signaling by platelet-derived growth factor-CC promotes tumor growth by recruitment of cancer-associated fibroblasts. Cancer Res 2009;69:369–78.
23. Pietras K, Pahler J, Bergers G, Hanahan D. Functions of paracrine PDGF signaling in the proangiogenic tumor stroma revealed by pharmacological targeting. PLoS Med 2008;5:123–138:e19.
24. Willett CG, Boucher Y, Duda DG, di Tomaso E, Munn LL, Tong RT, et al. Surrogate markers for antiangiogenic therapy and dose-limiting toxicities for bevacizumab with radiation and chemotherapy: continued experience of a phase I trial in rectal cancer patients. J Clin Oncol 2005;23:8136–39.
25. Rosen LS, Kurzrock R, Mulay M, Van Vugt A, Purdom M, Ng C, et al. Safety, pharmacokinetics, and efficacy of AMG 706, an oral multikinase inhibitor, in patients with advanced solid tumors. J Clin Oncol 2007;25:2369–76.
26. Rini BI, Michaelson MD, Rosenberg JE, Bukowski RM, Sosman JA, Stadler WM, et al. Antitumor activity and biomarker analysis of sunitinib in patients with bevacizumab-refractory metastatic renal cell carcinoma. J Clin Oncol 2008;26:3743–48.
27. Motzer RJ, Michaelson MD, Redman BG, Hudes GR, Wilding G, Figlin RA, et al. Activity of SU11248, a multitargeted inhibitor of vascular endothelial growth factor receptor and platelet-derived growth factor receptor, in patients with metastatic renal cell carcinoma. J Clin Oncol 2006;24:16–24.
28. Ivy SP, Wick JY, Kaufman BM. An overview of small-molecule inhibitors of VEGFR signaling. Nat Rev Clin Oncol 2009;6:569–79.
29. Franklin MC, Carey KD, Vajdos FF, Leahy DJ, de Vos AM, Sliwkowski MX. Insights into ErbB signaling from the structure of the ErbB2-pertuzumab complex. Cancer Cell 2004;5:317–28.
30. Badache A, Hynes NE. A new therapeutic antibody masks ErbB2 to its partners. Cancer Cell 2004;5:299–301.
31. Nahta R, Hung MC, Esteva FJ. The HER-2-targeting antibodies trastuzumab and pertuzumab synergistically inhibit the survival of breast cancer cells. Cancer Res 2004;64:2343–46.
32. Carmeliet P, Moons L, Luttun A, Vincenti V, Compernolle V, De Mol M, et al. Synergism between vascular endothelial growth factor and placental growth factor contributes to angiogenesis and plasma extravasation in pathological conditions. Nat Med 2001;7:575–83.
33. Autiero M, Waltenberger J, Communi D, Kranz A, Moons L, Lambrechts D, et al. Role of PlGF in the intra- and intermolecular cross talk between the VEGF receptors Flt1 and Flk1. Nat Med 2003;9:936–43.
34. Alam A, Herault JP, Barron P, Favier B, Fons P, Delesque-Touchard N, et al. Heterodimerisation with vascular endothelial growth factor receptor-2 (VEGFR-2) is necessary for VEGFR-3 activity. Biochem Biophys Res Commun 2004;324:909–15.
35. Ruch C, Skiniotis G, Steinmetz MO, Walz T, Ballmer-Hofer K. Structure of a VEGF-VEGF receptor complex determined by electron microscopy. Nat Struct Mol Biol 2007;14:249–50.
36. Yang Y, Xie P, Opatowsky Y, Schlessinger J. Direct contacts between extracellular membrane-proximal domains are required for VEGF receptor activation and cell signaling. Proc Natl Acad Sci U S A 2010;107:1906–11.
37. Tvorogov D, Anisimov A, Zheng W, Leppänen VM, Tammela T, Laurinavicius S, et al. Effective suppression of vascular network formation by combination of antibodies blocking VEGFR ligand binding and receptor dimerisation. Cancer Cell 2010;18:630–40.